Development, Factorial Optimization and In Vitro Release Evaluation of Montelukast Sodium-Loaded Chitosan Nanobiocomposites Prepared by Microwave-Assisted Processing

Manoj N. Phadtare[1,2*], Prajakta P. Shedage[2], Vaishnavi A. Mane[3], Supriya S. Pandhare[4], Tanuja N. Kashid[4], Priti S. Kolpe[5]

*[1] PhD in Pharmaceutical Sciences, Lords University, Alwar, Rajasthan, 301001, mnppharma1@gmail.com

[2]Sou.Venutai Chavan Pharmacy College Phaltan, Satara chemopharma29@gmail.com

[3]Krishna Institute of Pharmacy, Krishna Vishwa Vidyapeeth (Deemed to be University) Karad, vaishnavim1530@gmail.com, 0009000238371299

[4]Shri Ganpati Institute of Pharmaceutical Sciences Research, Tembhurni, Solapur , supriyapandhare999@gmail.com, kashidtanuja777@gmail.com

[5]DKSS, Dattakala Institute of Pharmaceutical Science and Research, Swami Chincholi, Dound, Pune, pritikolpe15@gmail.com

***Corresponding Author:**
Manoj N. Phadtare
PhD in Pharmaceutical Sciences
Lords University, Alwar,
Rajasthan, 301001,
mnppharma1@gmail.com

Abstract

Montelukast sodium is clinically useful in asthma but its low aqueous solubility can constrain dissolution and formulation performance. This study developed a chitosan-based nanobiocomposite using ionic cross-linking with sodium tripolyphosphate followed by controlled microwave processing. A three-level, two-factor factorial design examined chitosan concentration and the chitosan-to-TPP mass ratio. Entrapment efficiency, particle size and zeta potential were treated as critical quality attributes. Nine batches were compared, and NB6 combined the highest observed entrapment efficiency (84.6 ± 1.7%) with the smallest mean particle size (172.6 ± 4.2 nm) and a positive zeta potential of 31.8 ± 1.1 mV. Drug release from the optimized material reached 91.2 ± 2.1% at 24 h and was described most closely by first-order and Higuchi models (R^2 0.968 and 0.960, respectively). The results show that polymer content and cross-linker ratio jointly govern nanoparticle compactness, drug retention and release. The work supports NB6 as a formulation-development lead, while scale-up, aerosol performance, stability and confirmatory pharmacokinetic testing remain necessary.

Keywords: montelukast sodium; chitosan; nanobiocomposite; microwave-assisted synthesis; factorial design; controlled release

How to cite this article: Manoj N. Phadtare12* Prajakta P. Shedage2 Vaishnavi A. Mane3 Supriya S. Pandhare4 Tanuja N. Kashid4 Priti S. Kolpe5. Development, Factorial Optimization and In Vitro Release Evaluation of Montelukast Sodium-Loaded Chitosan Nanobiocomposites Prepared by Microwave-Assisted Processing. Int J Drug Deliv Technol. 2026;16(90s):384-389. DOI: 10.25258/ijddt.16.90s.38.

1. Introduction

Asthma is sustained by airway inflammation, variable bronchoconstriction and heightened responsiveness to environmental or biological triggers. Montelukast sodium blocks cysteinyl leukotriene type 1 receptors and is used as maintenance therapy rather than as a rescue medicine. A formulation that disperses the drug efficiently and moderates its release may improve consistency of exposure without changing its pharmacological target.

Chitosan is a cationic, biodegradable polysaccharide whose amino groups become protonated in acidic media. Those groups permit ionic association with multivalent anions such as tripolyphosphate, allowing nanoparticles to form under comparatively mild conditions. The same surface charge can promote interaction with negatively

charged mucosal components, although charge, size and polymer concentration must be balanced to avoid aggregation or excessive viscosity (Illum, 1998; Bhumkar & Pokharkar, 2006).

Microwave energy can shorten processing by producing rapid, volumetric heating. In a nanoparticle workflow, however, power and exposure must be controlled because local overheating can alter polymer chains or drug integrity. The present investigation therefore coupled ionic gelation with a bounded microwave step and used a factorial design to interpret formulation effects instead of selecting a batch from one-factor-at-a-time trials.

Quality-by-design thinking begins with a target product profile and links material attributes and process parameters to measurable outputs. For the current platform, entrapment efficiency indicates how successfully drug is retained, hydrodynamic diameter affects dispersion and biological interaction, and zeta potential provides an indirect measure of electrostatic stabilization. Release kinetics adds a functional test that connects structure with expected performance.

The objective was to prepare montelukast-loaded chitosan nanobiocomposites, quantify the influence of chitosan concentration and chitosan:TPP mass ratio, identify a balanced optimized batch, and characterize its release behavior. The dataset was taken from the attached thesis and is reported as a formulation-focused manuscript; animal efficacy outcomes are intentionally reserved for a separate article.

2. Materials and Methods

Montelukast sodium was obtained from Yarrow Pharmaceutical, Mumbai. Chitosan served as the polymer, sodium tripolyphosphate as ionic cross-linker, crosspovidone as stabilizing excipient, polyethylene glycol 400 as plasticizer and citric acid as a pH-adjusting component. Analytical-grade solvents and purified water were used throughout.

Identity testing included capillary melting point, ultraviolet spectrophotometry, Fourier-transform infrared spectroscopy and differential scanning calorimetry. The absorption maximum was established by scanning a suitably diluted solution from 200 to 400 nm. Calibration standards were prepared in phosphate buffer and analyzed at 345 nm. Linearity was checked by ordinary least-squares regression of absorbance against concentration.

For FTIR assessment, drug, polymer and drug-polymer preparations were dispersed in dry potassium bromide and scanned between 4000 and 400 cm-1. Characteristic bands were compared for retention, displacement or emergence of signals. DSC samples were sealed in aluminium pans and heated under nitrogen at 10°C/min over a range sufficient to capture the drug transition and polymer-related thermal events.

Chitosan was dissolved in 1% v/v acetic acid under stirring. Montelukast sodium was dispersed into the polymer solution, after which 0.1% w/v TPP was added dropwise under continuous mixing to initiate ionic gelation. Crosspovidone and PEG 400 were incorporated before the dispersion underwent a controlled microwave exposure within the thesis-defined ranges of 100-800 W, 30-300 s and 40-80°C. Nanoparticles were isolated by refrigerated centrifugation, washed and redispersed. The selected batch was pre-frozen and lyophilized.

A 3^2 factorial design investigated chitosan concentration at 0.10, 0.25 and 0.40% w/v and chitosan:TPP mass ratio at 1.5, 2.5 and 3.5. Nine experimental batches were produced. Responses were entrapment efficiency, particle size and zeta potential. The preferred region combined high entrapment, smaller size and an absolute surface potential compatible with dispersion stability.

Entrapment was measured indirectly. Dispersions were centrifuged at 15,000 rpm for 30 min at 4°C, and free montelukast in the supernatant was quantified at 345 nm. Entrapment efficiency was calculated as the difference between added and free drug divided by the added drug, multiplied by 100. Measurements were performed in triplicate.

Dynamic light scattering at 25°C and a backscatter angle of 173° provided the intensity-weighted hydrodynamic diameter. Electrophoretic mobility was measured in a folded capillary cell and converted to zeta potential. Triplicate results are expressed as mean ± standard deviation. A polydispersity index at or below 0.30 was considered supportive of a relatively narrow distribution.

For release testing, the optimized formulation was placed in a dialysis membrane system against phosphate buffer maintained at physiological temperature. Samples were removed at predetermined intervals and replaced with fresh medium. Drug concentration was determined spectrophotometrically, cumulative release was corrected for sampling, and profiles were fitted to zero-order, first-order, Higuchi and Korsmeyer-Peppas equations (Fu & Kao, 2010).

3. Results

The observed melting point was 136°C, close to the reference value of 135.5°C. The UV method produced increasing absorbance over 5-35 µg/mL, supporting its use for routine quantification. FTIR retained the principal drug- and chitosan-associated bands without a new dominant signal, while thermal analysis supported physical incorporation rather than obvious chemical degradation.

Table 1. Factor levels used in the 3² design

Factor	Low (-1)	Middle (0)	High (+1)
Chitosan (% w/v)	0.10	0.25	0.40
Chitosan:TPP ratio	1.5	2.5	3.5

Table 2. Formulation responses (mean ± SD, n = 3)

Batch	Chitosan	Ratio	EE (%)	Size (nm)	ZP (mV)
NB1	0.25	2.5	68.4 ± 2.1	225.4 ± 5.6	+22.5 ± 1.2
NB2	0.40	1.5	72.1 ± 1.9	218.3 ± 4.8	+24.3 ± 1.5
NB3	0.25	3.5	75.8 ± 2.4	210.7 ± 6.2	+26.1 ± 1.3
NB4	0.10	2.5	70.2 ± 2.0	221.8 ± 5.1	+23.6 ± 1.0
NB5	0.40	3.5	80.5 ± 1.8	189.5 ± 4.5	+29.4 ± 1.2
NB6	0.25	2.5	84.6 ± 1.7	172.6 ± 4.2	+31.8 ± 1.1
NB7	0.10	1.5	69.6 ± 2.2	223.7 ± 5.4	+22.9 ± 1.3
NB8	0.10	3.5	77.3 ± 1.9	204.8 ± 4.9	+27.5 ± 1.2
NB9	0.40	2.5	82.2 ± 1.6	181.4 ± 4.1	+30.2 ± 1.0

Table 3. Cumulative release from NB6

Time (h)	Cumulative release (%)
0.5	12.5 ± 1.2
1	20.4 ± 1.5
2	32.1 ± 1.8
4	46.8 ± 2.0
6	58.9 ± 2.2
8	68.7 ± 2.3
12	79.4 ± 2.4
24	91.2 ± 2.1

Table 4. Release-model comparison

Model	Rate parameter	R^2
Zero order	k0 = 5.107	0.297
First order	k1 = 0.144	0.968
Higuchi	kH = 21.101	0.960
Korsmeyer-Peppas	n = 0.47	0.949

Across the factorial batches, entrapment efficiency ranged from 68.4 ± 2.1% to 84.6 ± 1.7%. Mean particle size ranged from 172.6 ± 4.2 to 225.4 ± 5.6 nm, and zeta potential ranged from +22.5 ± 1.2 to

+31.8 ± 1.1 mV. NB6 delivered the most favorable simultaneous response profile.

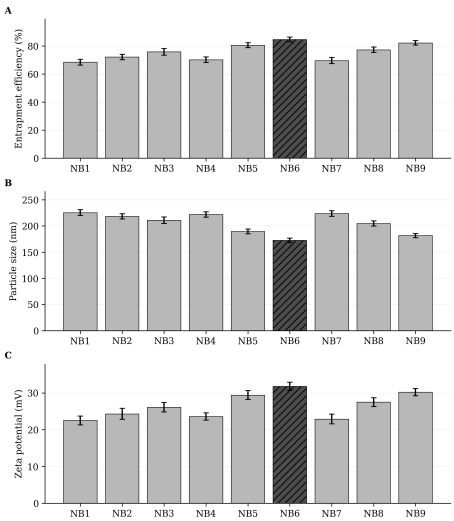


Figure 1. Responses of NB1–NB9: (A) entrapment efficiency, (B) particle size and (C) zeta potential.

The optimized formulation showed an initial release of 12.5 ± 1.2% at 0.5 h, followed by a progressive increase to 91.2 ± 2.1% at 24 h. The early fraction can be attributed to drug located near the particle surface, whereas the slower phase is consistent with diffusion through, and relaxation of, the cross-linked polymeric matrix.

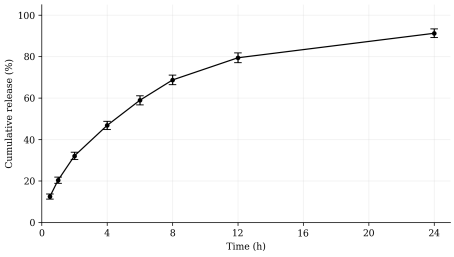


Figure 2. Cumulative montelukast release from NB6, plotted

Model comparison favored first-order behavior (R^2 0.968) with a closely comparable Higuchi fit (R^2 0.960). Zero-order fit was weak (R^2 0.297). The Korsmeyer-Peppas exponent of 0.47 indicated predominantly diffusion-associated release with a possible contribution from polymer relaxation.

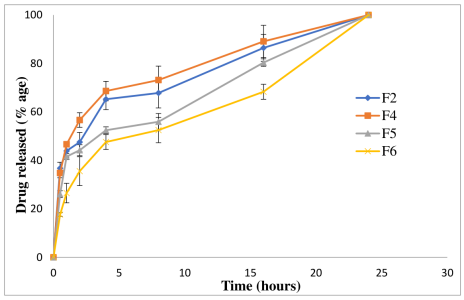


Figure 4. comparison of montelukast release from chitosan nanoparticle formulations.

Microwave assistance offers process efficiency, yet it introduces additional variables including vessel geometry, load volume, field distribution and cooling rate. These factors can alter local temperature even when nominal power is unchanged. A scale-up strategy should therefore specify energy delivered per unit mass, real-time temperature monitoring and maximum exposure rather than relying only on appliance power.

Compatibility findings are reassuring but not definitive proof of chemical stability. FTIR band retention mainly excludes large structural changes, and DSC peak modification can reflect dilution, amorphization or polymer interaction. A stability-indicating chromatographic assay and impurity profile are required to distinguish benign physical transitions from low-level degradation.

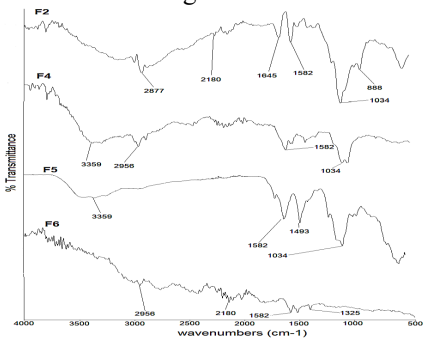


Figure 5. FTIR spectra of montelukast-loaded chitosan formulations

4. Discussion

Increasing chitosan does not produce a uniformly beneficial effect. More polymer can provide additional binding sites and raise drug retention, but it also increases solution viscosity and can enlarge particles if mixing and cross-linking become inefficient. TPP ratio likewise controls network density: insufficient cross-linker yields a loose matrix, whereas excessive cross-linker may produce local over-cross-

linking or aggregation. The response pattern therefore supports optimization of the factor combination rather than maximization of either factor alone.

The positive zeta potential arises from residual protonated amino groups on chitosan. Values around +30 mV are commonly interpreted as supportive of electrostatic repulsion, although zeta potential cannot by itself prove long-term physical stability. The modest particle diameter of NB6 may assist reproducible dispersion and creates a large surface area, but aerodynamic behavior must be measured before claims about respirability or regional lung deposition can be made.

The two-phase release profile is mechanistically plausible for an ionically cross-linked matrix. Loosely associated surface drug can partition rapidly into the medium, while entrapped molecules encounter a longer diffusional pathway. The strong first-order fit indicates concentration dependence, and the Higuchi fit shows that square-root-of-time diffusion also describes much of the profile. Model fitting should be interpreted descriptively because several equations can fit a limited set of time points.

5. Conclusion

Microwave-assisted ionic gelation produced montelukast sodium-loaded chitosan nanobiocomposites with formulation-dependent size, surface charge and entrapment. NB6 was the most balanced batch, achieving 84.6 ± 1.7% entrapment, 172.6 ± 4.2 nm particle size and +31.8 ± 1.1 mV zeta potential. Its sustained 24-h release and diffusion-associated kinetic behavior justify further development. Confirmation should include validated assay and impurities, aerosol performance, storage stability, scale-up robustness and pharmacokinetic comparison.

6. Declarations

Source of data: The numerical results were reorganized from the attached thesis, Final thesis by R B Misal. No new experimental observations were invented for this manuscript. Funding, conflict-of-interest, ethics approval and author-contribution statements should be completed by the submitting authors from the original institutional records before journal submission.

References

1. Bhumkar, D. R., & Pokharkar, V. B. (2006). Studies on the effect of pH on cross-linking of chitosan with sodium tripolyphosphate. AAPS PharmSciTech, 7(2), Article 50.
2. Fu, Y., & Kao, W. J. (2010). Drug release kinetics and transport mechanisms of polymeric delivery systems. Expert Opinion on Drug Delivery, 7(4), 429-444.
3. Illum, L. (1998). Chitosan and its use as a pharmaceutical excipient. Pharmaceutical Research, 15, 1326-1331.
4. Lehr, C. M., Bouwstra, J. A., Schacht, E. H., & Junginger, H. E. (1992). In vitro evaluation of mucoadhesive properties of chitosan and other natural polymers. International Journal of Pharmaceutics, 78, 43-48.
5. Panyam, J., & Labhasetwar, V. (2003). Biodegradable nanoparticles for drug and gene delivery to cells and tissue. Advanced Drug Delivery Reviews, 55, 329-347.
6. Van der Lubben, I. M., Verhoef, J. C., Borchard, G., & Junginger, H. E. (2001). Chitosan and its derivatives in mucosal drug and vaccine delivery. Advanced Drug Delivery Reviews, 52, 139-144.
7. Desai, M. P., Labhasetwar, V., Walter, E., Levy, R. J., & Amidon, G. L. (1997). Size-dependent uptake of biodegradable microparticles in Caco-2 cells. Pharmaceutical Research, 14, 1568-1573.
8. Gao, L., Zhang, D., & Chen, M. (2008). Drug nanocrystals for poorly soluble drugs and their application as delivery systems. Journal of Nanoparticle Research, 10, 845-862.
9. Chithrani, B. D., Ghazani, A. A., & Chan, W. C. W. (2006). Size and shape dependence of nanoparticle uptake into mammalian cells. Nano Letters, 6(4), 662-668.
10. Chen, M., Liu, Y., Yang, W., Li, X., Liu, L., & Zhou, Z. (2011). Self-assembled nanoparticles of cholesterol-modified chitosan for drug delivery. Carbohydrate Polymers, 84, 1244-1251.
11. Kawashima, Y., Handa, T., Takenaka, H., Lin, S. Y., & Ando, Y. (1985). Controlled-release granules

coated with a sodium polyphosphate-chitosan complex. Journal of Pharmaceutical Sciences, 74, 264-268.

12. Ma, Z., Yeoh, H. H., & Lim, L. Y. (2002). Formulation pH modulates drug interaction with chitosan nanoparticles. Journal of Pharmaceutical Sciences, 91, 1396-1404.